HHS Public Access

Author manuscript

Mol Pharm. Author manuscript; available in PMC 2021 December 07.

Published in final edited form as:

Mol Pharm. 2020 December 07; 17(12): 4691–4703. doi:10.1021/acs.molpharmaceut.0c00983.

Local Targeting of Lung Tumor Associated Macrophages with Pulmonary Delivery of a CSF-1R Inhibitor for the Treatment of Breast Cancer Lung Metastases

Sulaiman S. Alhudaithi[1,&], **Rashed M. Almuqbil**[1,^], **Hanming. Zhang**[1], **Elizabeth Bielski**[1,%], **Wei. Du**[2], **Fatemah Sunbul**[1], **Paula Bos**[2,3], **Sandro R. P. da Rocha**[1,3,*]

[1]Department of Pharmaceutics and Center for Pharmaceutical Engineering and Sciences, School of Pharmacy, Virginia Commonwealth University, Richmond 23298, Virginia, United States

[2]Department of Pathology, School of Medicine, Virginia Commonwealth University, Richmond 23298, Virginia, United States

[3]VCU Massey Cancer Center, School of Medicine, Virginia Commonwealth University, Richmond 23298, Virginia, United States.

Abstract

The lungs are major sites of metastases for several cancer types, including breast cancer (BC). Prognosis and quality of life of BC patients that develop pulmonary metastases are negatively impacted. The development of strategies to slow the growth and relieve the symptoms of BC lung metastases (BCLM) is thus an important goal in the management of BC. However, systemically administered first line small molecule chemotherapeutics have poor pharmacokinetic profiles and biodistribution to the lungs, as well as significant off-target toxicity, severely compromising their effectiveness. In this work we propose the local delivery of an add-on immunotherapy to the lungs to support first line chemotherapy treatment of advanced BC. In a syngeneic murine model of BCLM we show that local pulmonary administration (p.a.) of PLX-3397 (PLX), a colony stimulating factor 1 receptor inhibitor (CSF-1Ri), is capable of overcoming physiological barriers of the lung epithelium, penetrating the tumor microenvironment (TME), and decreasing phosphorylation of CSF-1 receptors, as shown by western blot of lung tumor nodules. That inhibition is accompanied by an overall decrease in the abundance of pro-tumorigenic (M2-like) macrophages in the TME, with a concomitant increase in the amount of anti-tumor (M1-like) macrophages when compared to vehicle treated control. These effects with PLX p.a. were

*to whom correspondence should be addressed: srdarocha@vcu.edu.

&Doctoral student, VCU Department of Pharmaceutics. Faculty on leave from the Department of Pharmaceutics, College of Pharmacy, King Saud University, Riyadh, Saudi Arabia

^Doctoral student, VCU Department of Pharmaceutics. Faculty on leave from Department of Pharmaceutical Sciences, College of Clinical Pharmacy, King Faisal University, Al Ahsa, Saudi Arabia

%Current position: Chemist in the Division of Therapeutic Performance (DTP)/ORS/OGD at FDA - Orally Inhaled Drug Products

SUPPORTING INFORMATION

The Supporting Information is available free of charge at https://doi.org/10.1021/acs.molpharmaceut.0c00983

Assessment of tdTomato expression on transduced 4T1 cells via Flow-cytometry; *In vitro* kinetics of luc-tdT 4T1 cells; Assessment of Puromycin cytotoxicity via MTT assay; Assessment of PTX cytotoxicity via MTT assay; Assessment of lung deposition in animals after endotracheal intubation; *In vivo* biolumenscince of mice on day zero after tail vein injection of luc-tdT 4T1 cells; Total flux of treatment groups as measured by *in vivo* bioluminescence analysis of mice on day 7; Measurement of body weights of mice treated with 1 x PBS; Gating strategy for M1 TAMs on Flow- cytometry for tumor samples (PLX, PTX, and PLX+PTX groups) (PDF)

achieved using a much smaller dose (1 mg/kg, every other day) compared to the systemic doses typically used in preclinical studies (40–800 mg/kg/day). As an additive in combination with intravenous (i.v.) administration of paclitaxel (PTX), p.a. PLX leads to a decrease in tumor burden without additional toxicity. These results suggested that the proposed immunochemotherapy, with regional pulmonary delivery of PLX along with i.v. standard of care chemotherapy, may lead to new opportunities to improve treatment, quality of life, and survival of patients with BCLM.

Graphical Abstract

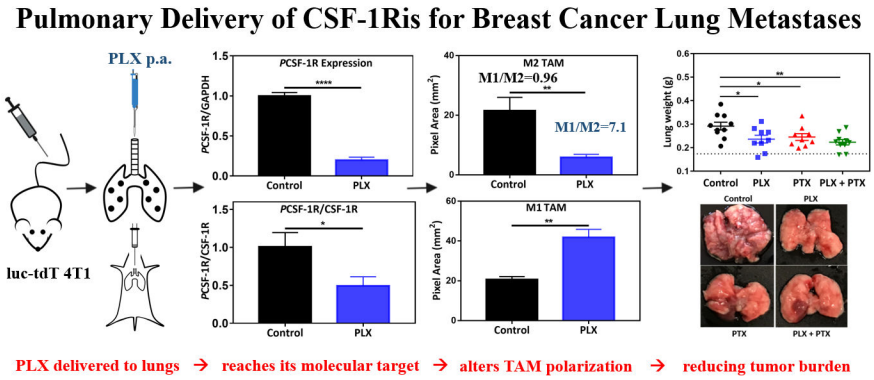

Keywords

Breast Cancer Lung metastases (BCLM); Combination therapy; Tumor associated macrophages (TAMs); Colony stimulating factor 1 receptor inhibitor (CSF-1Ri); PLX-3397 (PLX); Paclitaxel (PTX); immunotherapy

1. INTRODUCTION

Cancer cells can invade surrounding tissues and traffic through the vascular or lymphatic systems and establish in distant organs, a process known as metastasis[1]. Cancer metastases contribute to 90% of cancer-related deaths[2], and the lungs are one of the primary sites of metastases for several cancers, including breast cancer (BC)[3,4]. Pulmonary metastases are detected in 60–70% of patients who die with metastatic BC[5], and the lungs represent the first site of distant metastasis in 40% of women with recurrent triple negative BC (TNBC)[6]. This statistic is relevant as the overall survival (OS) of TNBC patients with pulmonary metastases is markedly lower compared to individuals with non-pulmonary tumors[7].

There are few treatment options for patients with advanced TNBC, with chemotherapy being one of the most prominent regimens[8–10]. Unfortunately, first line small molecule chemotherapeutics typically used in the management of advanced TNBC have high off-target toxicity[11], as well as poor pharmacokinetic (PK) and lung tumor biodistribution profiles[12]. Furthermore, such treatment regimens are largely ineffective in addressing pulmonary metastases[12], while negatively impacting the quality of life of BC patients[13].

Several new approaches have been recently devised to support the treatment of TNBC patients by leveraging the patient's own immune system[14,15]. An antibody-drug conjugate

(Atezolizumab-nab paclitaxel) has been approved by the FDA for use in TNBC patients[14], giving new hope for TNBC survivors. Atezolizumab belongs to a class of drugs known as immune-checkpoint inhibitors (ICI) and works by targeting programmed death-ligand 1 (PD-L1), which is highly expressed in certain cancers and interacts with PD-1 or B71 on CD8 cytotoxic T cells, delivering a negative signal to their activation[16]. Atezolizumab blocks the PD-1 - PD-L1 binding, reversing CD8 T cell exhaustion, thereby re-invigorating T cell-mediated tumor cell killing[17]. However, antibody therapy is only indicated for patients with high expression of PD-L1, which represents approximately 41% of individuals with TNBC[14]. Antibody therapy is unfortunately not free of adverse effects either, including systemic toxicity[14,18]. Resistance to ICI[19,20] has also emerged as significant challenge. In fact, more recently, FDA has released an alert regarding efficacy and potential toxicity associated with the use of atezolizumab in combination with paclitaxel for treatment of breast cancer, and indicated that continuous approval of the conjugated therapy may be granted if additional clinical trials prove it is beneficial[21].

Another promising form of immunotherapy for the treatment of solid tumors including BC is the reprograming of tumor-associated macrophages (TAMs) with colony stimulating factor 1 (CSF-1) receptor inhibitors (CSF-1Ris)[22–24]. The first CSF-1Ri has been approved by the FDA in 2019[25], and several clinical trials are ongoing[26–28]. TAMs are abundant in the complex solid tumor microenvironment (TME)[29,30], and along with other immune infiltrates contribute to signaling that lead to tumor invasion, progression, and metastasis[22,31,32]. Monocytes and macrophages are recruited to the TME primarily in response to CCL2 (also known as monocyte chemotactic protein-1, MCP-1) and colony stimulating factor 1 (CSF-1)[23,33]. Macrophages, as a result of different microenvironmental cues emanating from the TME, differentiate into a spectrum of different phenotypes comprised between two extremes with opposing functions: classically activated (M1-like) and alternatively activated (M2-like) macrophages[23]. In cancer, M2-like TAMs are generally associated with immunosuppression, play a central role in angiogenesis and metastasis, and are induced by factors like hypoxia, CSF-1, IL-4, and IL-10[22,34]. On the other side of the spectrum, the M1-like TAM phenotype is pro-inflammatory in nature, promote tumoricidal functions[23,35,36], and it is induced by factors like IFNγ, TNFα, IL-12, and lipopolysaccharide (LPS)[22,34].

CSF-1R is a type III receptor tyrosine kinase highly expressed in macrophages[37], and when binding to its primary ligand, CSF-1, it activates signalling pathways that lead to macrophage recruitment into inflammatory sites and polarization[38,39]. Inhibition of this axis, via either antibodies or small molecules, has been shown to prevent tumor recruitment and/or shift macrophages balance from the M2-like to the M1-like tumor-killing phenotype, leading to an increase in M1/M2 ratio[40–45]. A high M1/M2 ratio has been correlated with positive clinical outcomes[42,44,45], including in BC patients[46]. Pexidartinib (PLX-3397, PLX hereafter) is a small molecule with high affinity to CSF-1R, and is currently being studied in clinical trials for breast cancer, melanoma, and other advanced solid tumors[26,28,47]. PLX has been approved for treatment of a rare, non-malignant disease, tenosynovial giant cell tumor (TGCT)[25], which is characterized by overexpression of CSF-1, leading to a strong recruitment of macrophages that localize around neoplastic cells, developing massive tumors[48]. Although systemic administration of PLX has indicated promising outcomes in blunting tumor progression, many clinical studies linked the molecule with hepatotoxicity

that varies from mild, reversible (low grade) toxicity to serious irreversible liver damage[49–51] as a consequence of its action on Kupffer cells. This may represent a potential limitation in systemic use of such immunomodulators to support chemotherapy and antibody therapies[49,51], which have high toxicity profile on their own.

Based on the challenges and opportunities of combination immune-chemotherapy in the treatment of BCLM, the purpose of this work was to evaluate the potential of local administration of a CSF-1Ri (PLX) to the lungs in shifting the M1/M2 TAM ratio, and to study its efficacy as an add-on treatment to first line chemotherapy (paclitaxel, PTX) in an *in vivo* model of triple-negative breast cancer lung metastasis (TNBCLM). Local lung administration of such small molecule immunomodulators may help overcome their poor biodistribution to the lung tumors typically observed upon systemic administration, and with improved drug deposition, to decrease required total dose, and consequently their unwanted off-target toxicity[52–54]. Such route of administration may also allow for the outpatient use of this add-on therapy in the treatment of BCLM as formulation in portable inhalers is explored.

2. MATERIALS AND METHODS

2.1 Materials

Wild Type 4T1 cells (WT 4T1) were obtained as a kind gift from Dr. Rishi (Department of Oncology at Wayne State University). Dulbecco's modified Eagle's medium (DMEM) 1x high glucose with sodium pyruvate (Gibco™), RPMI Medium 1640 (Gibco™), and penicillin-streptomycin antibiotics 100x (Gibco™) were purchased from ThermoFisher. Fetal bovine serum (FBS) and Liberase TL Research Grade (Roche) were obtained from Sigma-Aldrich. Trypsin EDTA 1x and puromycin dihydrochloride were supplied by Corning®. 24 and 96-well culture plates were purchased from Thomas Scientific. D-Luciferin Potassium Salt was obtained from Syd labs (Southborough, MA). Paclitaxel (PTX) was supplied by LC Laboratories and PLX was purchased from CHEMGOOD. MTT (Thiazolyl Blue Tetrazolium Bromide) was purchased from Research Products International (Mount Prospect, IL). Isoflurane, USP was obtained from VetUS™. Tissue Protein Extraction Reagent (T-PER), protease and phosphatase inhibitor cocktail, Pierce BCA Protein Assay Kit, and GAPDH loading control monoclonal antibody (catalog #MA5-15738) were purchased from Thermo Scientific™. Clarity Western ECL Substrate, 10% Mini-PROTEAN TGX Stain-Free Protein Gels, 10x Tris Buffered Saline (TBS), Trans-Blot Turbo RTA transfer kit were obtained from Bio-Rad. M-CSF receptor antibody (#3152), phospho-M-CSF receptor antibody (#3155), Anti-rabbit IgG, HRP-linked Antibody (#7074), and Anti-mouse IgG, HRP-linked Antibody (#7076, a kind gift from Dr. McClay, VCU) were supplied by Cell Signaling Technology®. OCT compound was obtained from Sakura Finetek (Torrance, CA) and positively charged glass slides were purchased from Globe Scientific. TruStain FcX™ PLUS (anti-mouse CD16/32, catalog# 156603), True-Nuclear™ Transcription Factor Buffer Set (catalog# 424401), Brilliant Violet 421™ anti-mouse F4/80 Antibody (catalog# 123131), Zombie Aqua™ Fixable Viability Kit (catalog# 423101), FITC anti-mouse CD45 (catalog# 147709), APC/Fire™ 750 anti-mouse/human CD11b (catalog# 101261), PerCP-Cy5.5 anti-mouse I-A/I-E (catalog# 107625), Alexa Fluor® 488 anti-mouse

I-A/I-E (kind gift, catalog# 107615), FITC anti-mouse CD80 (catalog# 104705), and Alexa Fluor® 488 anti-mouse CD206 (catalog# 141709) were obtained from BioLegend®.

2.2. Methods

2.2.1. Cell Culture.—WT 4T1 cells were grown using DMEM media supplemented with 10% FBS and 1% penicillin-streptomycin antibiotics (AB) and cultured at 37 °C and 5% CO_2. Puromycin (4 μg/ml) was added to the media used to culture stably transfected luciferase (luc)-tdTomato (tdT) 4T1 cells (luc-tdT 4T1 cells), which were established as discussed next.

2.2.2. luc-tdT 4T1 Cell Development.—4T1 cells were modified to express firefly luciferase and tdTomato, according to modified protocols from GenTarget and provided by Dr. Yemelyanov and Dr. Bhalla from Northwestern University. Briefly, 25,000 4T1 cells (Passage 14) were seeded in each well of a 24-well microplate cultured with 500 μL of DMEM supplemented with 10% FBS and 1% AB at 37°C and 5% CO_2. The following day, they were transduced with 10^{10} TU/ml of a lentivirus containing luc and tdT (pFULT Ubi>Luciferase-T2A-tdT, Skin Disease Research Center, Northwestern University) and 8 μg/ml polybrene, and incubated at 37°C and 5% CO_2 overnight. The following day, the medium containing the virus was replaced with fresh DMEM +10% FBS+ 1% AB for 2.5 hours. A second round of transduction was performed in the same conditions and cells were allowed to recover for additional 72 hours. Stably transduced cells were then selected in puromycin-containing medium (DMEM + 10% FBS + 4 μg/ml puromycin, based on a puromycin titration curve) to select for cells that express the lentivirus. Confluent cell cultures were then sorted twice using tdT fluorescence expression by fluorescence-activating cell sorting (FACS, SC Aria- BD FACSAria™ II High-Speed Cell Sorter, Flow Cytometry Shared Resource Core, Virginia Commonwealth University). After sorting, luc-tdT 4T1 cells were cultured in DMEM+10% FBS+1% AB+ 4 μg/ml puromycin. The expression of tdT by transduced cells was continuously monitored with flow cytometry (CytoFLEX Flow Cytometer, Beckman Coulter). To assess the expression of luc, and the kinetics of conversion of D-luciferin by the luc transformed cells *in vitro*, various densities of luc-tdT 4T1 cells (15625–250,000 cells) were seeded in wells of a 24-well microplate. A working solution of D-luciferin (luciferase substrate, 150 μg/ml) was added to each well 20 min after seeding, and bioluminescent imaging (BLI) was assessed at 5, 10, 15, and 20 min time points using *In vivo* Imaging System (Xenogen IVIS Spectrum, Microscopy Core, Virginia Commonwealth University) and Living Image® 4.5.5 Software (PerkinElmer) for image analysis.

2.2.3. Cell Viability Assay.—4T1 cells (1×10^4) were seeded in each well of 96-well plates and cultured in DMEM+10%FBS+1%AB at 37°C and 5% CO_2 overnight. Multiple concentrations of puromycin (0.5, 1, 2, 4, 6, 8, and 10 μg/ml) or PTX (0.01, 0.1, 1, 10, 25, 50, 75, and 100 μM) were prepared by solubilizing in H_2O (puromycin) or 0.13% v/v DMSO (PTX), diluted in the respective medium, and added to the wells for 48h at 37°C and 5% CO_2. 0.13% (v/v) DMSO in the medium was not toxic to cells (data not shown). Cells then were washed 2x with 1x PBS and 110 μL of 1.09 mM of MTT stock solution (dissolved in 1x PBS) was added to each well. The cells were incubated at 37°C and 5% CO_2 for 3–4h

and protected from light. A total volume of 85 μL was removed from each well and replaced by 60 μL DMSO. The plate was then incubated at 37°C and 5% CO_2 for 10 minutes. Absorbance was measured at 540nm using microplate reader (Synergy H1, BioTek). No drug treatment (0 μM puromycin or PTX wells) served as control, and their average absorbance was taken as 100% cell viability. Blank absorbance was subtracted from all other absorbance values and percentage viability was calculated with respect to the control readings (100%). Nonlinear fit of normalized data (log inhibitor vs normalized response) was generated to estimate IC_{50} values and the confidence interval (CI) for PTX.

2.2.4. Preclinical Tumor Model and Treatment Groups.—8–10-weeks old virgin female Balb/c mice were injected in the tail vein with 250k luc-tdT 4T1 cells to obtain a model of breast cancer lung metastases (BCLM). Shortly after cell inoculation, D-luciferin (150 mg/kg) was administered to each animal via subcutaneous injection (S.C.). Animals were maintained on isoflurane for 10 min prior to being imaged via *in vivo* BLI. Mice were then imaged with an IVIS Spectrum instrument (Xenogen) for 3 minutes. Data was plotted as sum of dorsal and ventral imaging of the thoracic area (Figure S6). Imaging at day 0 post inoculation (DPI = 0) was performed to evaluate accuracy of injection. On day 7, before any treatment, animals were subjected to *in vivo* BLI, and were then randomized based on lung metastatic burden and allocated into four independent groups and treatment initiated (Figure S7). Treatment continued for two weeks, with a regimen of three doses per week, every other day, and a repeat a week after. Groups of 9–10 animals were treated with (i) vehicle (1% DMSO and 5% Tween80 in 1x PBS) administered via pulmonary administration (p.a.), (ii) PLX (1 mg/kg, p.a. dissolved in 1% DMSO and 5% Tween80 in 1x PBS), (iii) PTX (1 mg/kg, i.v. dissolved in 1% DMSO and 5% Tween80 in 1x PBS), or (iv) PLX + PTX (1 mg/kg, p.a., and 1 mg/kg, i.v., respectively). The total volume administered via p.a. was adjusted to achieve the necessary dose per body weight, at ca. 25μL per dose. Pulmonary administration (p.a.) was performed utilizing an endotracheal intubation system (Kent Scientific). Animals were anesthetized via isoflurane before being placed onto an intubation stand linked with anesthesia mask (for continuous anesthesia) and were held by hooking up upper incisors with a small suture located at the top of the stand. Mice tongues were gently retracted, and a catheter was carefully inserted, over the epiglottis and between the arytenoid cartilages, into the larynx with the help of the fiber-optic light guide. Once the catheter was inserted, the light guide was quickly removed from the catheter to allow for normal breathing, and then therapeutics were added to the catheter for drug administration to the animals. After delivery of the drug solution, mice were placed in their cages, over a heating pad, and monitored until full recovery (ca. 5 min).

One day after the final treatment, the animals were sacrificed and lungs were excised, imaged *ex vivo* using BLI, and weighed to determine tumor burden. Lung weight was assessed after excision, brief rinsing in 1x DPBS, and gently tapping to remove excess liquid. Throughout the study, mice were monitored on a daily basis for signs of toxicity, including significant body weight loss (20% weight loss from day zero body weight), ungrooming, porphyrin staining around eyes and nostrils, hunched posture, respiratory distress, and changes in behavior (abnormal hyperactivity/hypoactivity, aggression, isolation). Body weight measurements were recorded over a 19-day period and are

represented as percentage changes. All animals were maintained at Massey Cancer Centre animal facilities, Virginia Commonwealth University, and all procedures were performed in compliance with the protocol AD10001431, approved by Institutional Animal Care and Use Committee (IACUC).

2.2.5. Western Blot—Tumor nodules were removed from lungs of treated animals, snap frozen in liquid nitrogen and stored at −80°C until use. When ready to process, tumor nodules were placed in 1.5 ml tubes containing T-PER buffer with 100X protease and phosphatase inhibitor cocktail, and total protein was extracted via homogenization. Protein in each sample was quantified using BCA assay. Western blotting was performed using wet transfer method. Briefly, protein lysates were separated with SDS-PAGE, transferred to PVDF membranes, and then blocked with 5% (w/v) nonfat milk in TBST for 30 minutes at RT. Membranes were incubated overnight with primary antibodies; M-CSF receptor rabbit (1:1000), Phospho-M-CSF receptor rabbit (1:1000), and GAPDH mouse (1:10000) mAbs. HRP-linked secondary antibodies (anti-rabbit, 1:3000, or anti-mouse, 1:10000) were added to blots for one hour at RT. Enhanced chemiluminescence substrate was applied to detect for bioluminescent signals using ChemiDoc™ Touch Imaging System. Protein bands were quantified using Image Lab™ software.

2.2.6. Immunofluorescence and Histology—Lung tumor nodules were extracted from the lungs of mice from the various treatment groups (n=3 per group). Tumor nodules were then enriched at 4°C in 10% sucrose (1h), then 20% sucrose (1h), and then in 30% sucrose overnight. Tumors were fixed in 4% paraformaldehyde (PFA) for 1h, and samples were placed in OCT compound and stored in −80°C until use. For immunofluorescence (IF) analysis, samples were blocked with 10% (v/v) FBS in 1x PBS at RT in dark humidified chamber for 1h before being stained with F4/80 (0.5μg/ml) and either CD206 or CD80 or MHCII (2.5μg/ml), and then diluted in 0.5% (w/v) BSA in 1xPBS, at RT in dark humidified chamber for 24h. Slides were imaged using a confocal microscope (ZEISS710, Shared microscopy core at Virginia Commonwealth University) at 10x and 63x magnification. Images at 10X were analyzed for M2-like (F4/80-CD206 overlay), M1-like (F4/80-CD80 overlay or F4/80-MHCII) phenotypes by using the co-localization threshold feature in ImageJ (FIJI) software. Pixel values for 6 random areas in each slide (imaged at 10X) were used, and those pixel values were converted to areas (1 pixel = 0.98 μm^2). Images at 63x were used for qualitative analyses. For histology, lungs were harvested from tumor bearing mice and snap frozen. Tissues were processed as for IF, and hematoxylin and eosin (H & E) staining was performed.

2.2.7. Flow-cytometry—Lung tumor nodules were extracted from the lungs of mice in the various treatment groups (n=3 mice per group). Tumor nodules were then chopped in presence of Liberase™ and the digestion mix was incubated at 37 °C for 25 min. Cells were filtered through 100 μm cell strainers and Fc receptors were blocked with anti CD16/32 for 10 min before being stained with zombie (live/dead) and anti-CD45, CD11b, F4/80, and MHCII antibodies in dark at 4°C for 30 min. Cells were fixed at RT for one hour, and were analyzed the following day using a flow cytometer (CytoFLEX).

2.2.8. Statistical Analyses.—Statistical analyses were performed using GraphPad Prism 7. Data are presented as mean ±SEM. The statistical tests performed are indicated in each figure and were utilized to estimate differences between groups. Differences of P value < 0.05 were considered statistically significant.

3. RESULTS

3.1. Stable Transduction of luc-tdT 4T1 Cells and their *in vitro* Sensitivity to Chemotherapy.

In this study we chose to use the 4T1 cell line, as it is an extensively characterized murine model of triple negative breast cancer used for *in vivo* preclinical TNBC research[55–58]. It is a particularly relevant model in our study as it exhibits high rates of pulmonary metastasis upon tail vein (i.v.) injection, thus allowing for efficient establishment of the BCLM model[59,60]. Importantly, it is syngeneic to Balb/c mice, thus representing an opportunity to study the proposed treatment strategies in an immunocompetent mouse model.

4T1 cells were transduced with lentivirus coding for Firefly Luciferase (luc) and TdTomato fluorescent protein (tdT) genes (pFULT Ubi > Luciferase-T2A-tdTomato Lentiviral stocks) to obtain luc-tdT 4T1 cells that allow the quantification of tumor burden *in vivo* and *ex vivo*. After transduction, luc-tdT 4T1 cells were selected with puromycin and sorted using FACS. Flow cytometry analysis demonstrated that >99% of 4T1 cells express tdT (Figure S1).

The tdT expression was also examined prior to each animal study as a quality assurance strategy. To verify the transduction efficiency of the luminescence gene and to assess kinetics of the conversion of luciferase, *in vitro* bioluminescence of luc-tdT 4T1 cells was assessed using an IVIS Imaging System (Figure S2). The cells expressed luciferase, and higher bioluminescence signals were seen as the cellular density increased. Transduced cells were cultured in medium with 4 μg/ml puromycin, as this concentration was determined to induce 100% cytotoxicity in WT 4T1 cells in about 2 days and sustained after selection to prevent outgrowth of non-selected clones (Figure S3).

Given the absence of known actionable target for therapy, chemotherapy is the main treatment modality in advanced TNBC[8–10]. Besides anthracyclines, paclitaxel (PTX) is a first line therapy for metastatic/recurrent disease, either as a monotherapy or in combination with Atezolizumab, a blocking antibody that prevents the activation of the T cell exhaustion pathway PD-1, indicated for women with unresectable, PD-L1$^+$ tumors[8–10,14]. PTX is a potent drug and belongs to the taxane family and induces cancer cell apoptosis by either interference with the cell cycle causing cellular arrest or through activation of the apoptotic toll-like receptor 4 (TLR4) signaling[61].

The cytotoxic property of PTX on 4T1 cells *in vitro* was thus examined utilizing MTT assay. PTX was able to induce WT 4T1 cellular toxicity, with an IC50 of 1.14 μM. Transduction of the WT 4T1 cells to express luc and tdT did not affect their susceptibility or sensitivity to PTX, with luc-tdT 4T1 cells presenting a similar IC50 of 1.55 μM (Figure S4), being in that regard suitable for the *in vivo* experiments.

3.2. Impact of Local Administration of Add-on TAM Immunotherapy Combined with Systemic Chemotherapy on Breast Cancer Lung Metastases Burden *in vivo*.

Given the prominent role of TAMs in breast cancer progression and metastasis[62], and the promise of CSF-1Ris in repolarizing TAMs towards an anti-tumorigenic phenotype, we set out to investigate whether a combination of PLX administered via p.a. as add-on to standard of care chemotherapy (PTX) administered i.v. would lead to a decrease in lung tumor burden in an immunocompetent BCLM model. The treatment timeline is shown in Figure 1A.

Single-agent treatment with CSF-1Ri or PTX resulted in a partial decrease in lung tumor burden, while combination therapy led to a significant reduction in tumor burden as measured by *ex vivo* BLI (Figure 1B). This observation was confirmed by measuring lung tumor burden by lung weight, with average lung weights of animals treated with single agents being significantly lower than control animals, and combination therapy resulting in further reduction in average lung weight (Figure 1C). Optical images of representative lungs are shown to complement the BLI and lung weight quantification, where far fewer and smaller lung nodules are observed for the combination therapy (Figure 1B–C, right panels).

In this study, all treatments, alone or in combination, were well tolerated, with no noticeable overt toxicity. There was no significant reduction in body weight (Figure 1D), and none of the various treatment regimens resulted in changes in behavior, fur appearance, movement, respiration and overall health. Treatment of mice with 1 x PBS resulted in similar outcomes as vehicle treated group, including body weight changes (Figure S8), indicating that 1% DMSO, 5% tween in 1x PBS is well tolerated and a suitable vehicle for these pre-clinical studies.

3.3. Ability of Locally Delivered PLX to the Lungs to Reach its Molecular Target

Ligation of CSF-1 to CSF-1R leads to chain dimerization and autophosphorylation of the intracellular tyrosine kinases, resulting in activation of the receptor[22,63]. PLX binds to the intracellular kinase domain of CSF-1R, leading to inhibition of phosphorylation and the associated downstream signaling pathways, thereby averting CSF-1/CSF-1R axis-mediated molecular effects[37].

To test the ability of PLX to reach and inhibit its molecular target upon pulmonary delivery, we performed western blot analysis on digested lung tumor nodules to specifically assess the effect on intra-tumoral macrophage population. Results (Figure 2) show that local pulmonary administration of PLX, leads to a significant decrease in phosphorylated CSF-1R (*P*CSF-1R, Figure 2C) and inhibition of CSF-1R activation (Figure 2D) when normalized to total receptor levels. PLX also partially reduced the unphosphorylated form, CSF-1R (Figure 2B), which is likely a consequence of inhibition of receptor activation – it causes a decrease in the abundance of M2-like TAMs which highly express CSF-1R[22,38]. Such effect was also seen in gliomas upon treatment with PLX[41].

3.4. Impact of Macrophage Immunotherapy and Chemotherapy on TAM Population

In order to study the role of CSF-1Ri in the TAM population in the TME, tumor nodules were sectioned and stained with the traditional murine macrophage marker F4/80, the

classical activation marker CD80 and the scavenger receptor CD206, typically associated with alternative activation of TAMs (Figure 3–4). Recruitment of TAMs into the lung TME was not significantly affected, since we observed similar density of F4/80+ TAMs in all treatment conditions (Figure 3C). Interestingly, inhibition of CSF-1R through local administration of PLX alone or in combination with i.v. PTX correlates with a marked decrease in the number of $F4/80^{+}$ $CD206^{+}$ TAMs (Figure 3D). Quantification of F4/80+ CD80+, indicative of classically activated M1-like TAMs, revealed that CSF-1Ri leads to an increase in the number of these TAMs (Figure 4B), demonstrating that local administration of PLX or PLX + systemic PTX combination results in an enhancement of the M1/M2 ratio (control:0.96, PLX: 7.1, PLX+PTX:4).

To confirm this observation, we analyzed the number of F4/80+ MHCII+ cells, also indicative of classically activated TAMs, by IF (Figure 5A–B) and flow cytometry (Figure 5C–D). Local PLX therapy, alone or in combination with systemic PTX, resulted in an increase in the number of $F4/80^{+}$ $MHCII^{+}$ TAMs both by IF (Figure 5B) and flow cytometry (Figure 5D). These results also indicate an increase in the antigen presentation capacity in TAMs, which may lead to improvement in the adaptive antitumor response, as macrophages can present tumor antigens to CD4 T cells through MHCII molecules[64]. M2-like TAMs are $MHCII^{low}$ and thus their tumor associated antigen presentation is inefficient[65].

4. DISCUSION

Immunotherapies have been extensively investigated for the treatment of variety of cancers[50,66–68] and have shown promising results in a small subset of patients with advanced breast cancer[14,69]. Immunotherapeutics, such as ICIs, are utilized in the clinic to treat lung cancers[70,71] and some advanced solid tumors featuring pulmonary metastases[71]. All those agents are administered systemically, and have associated off-target toxicity[54,72], with therapeutic efficacy in the treatment of pulmonary metastases being typically low. The problem is compounded for small molecules as their pharmacokinetic (PK) profiles are not favorable, and biodistribution to the lungs upon i.v. administration (or other non-local routes) is poor[73], being in the order of a few percent of the total dose.

Local administration of drugs to the lungs via oral inhalation (OI) has been shown to help minimize systemic toxicity and enhance biodistribution to the lung tissue[52,74–77], and thus offer an opportunity to develop innovative and safe add-on treatments for pulmonary metastases to support first line therapies[52,74,78]. Importantly, in spite of compromised lung function, several clinical studies have demonstrated that patients suffering from primary and secondary lung tumors can benefit from chemotherapy delivered via OI[74,79], and those treatments have acceptable toxicity profiles with several studies moving on to Phase II[80–82]. Clinical studies have also shown that such strategies are effective in reducing lung tumor burden[74,79], including lesions at distant sites[83]. In fact, aerosol based therapies for local lung delivery have been also extended to include clinical trials of a limited number of immunomodulators (IL-2 and granulocyte-macrophage CSF, GM-CSF), that were studied to target melanoma[52,84], renal carcinoma[78,85], and osteosarcoma pulmonary metastases[86]. Although some of those studies demonstrated positive therapeutic outcomes, they have not reached the market yet[78,85].

For pulmonary administered therapies (e.g. CSF-1Ris) to exert their action locally, they must overcome barriers that differ depending on the region of interest. In the upper airways, drug formulations should cross the mucus layer and avoid enzymatic degradation and clearance via the mucociliary escalator. Aerosolized drugs that target the alveolar region must also evade extensive clearance via alveolar macrophages, and demonstrate an adequate retention time in the lungs before being cleared through systemic absorption[87,88]. Pulmonary surfactants may also promote alveolar macrophage-mediated drug clearance by their interaction with drug particles[89]. If the target is the tumors in the lung tissue, such therapies need also to overcome tumor barriers[90]. Those include the tumor extracellular matrix (ECM), which offers opportunities for non-specific interactions with certain drug functionalities, as is the case of the protonated amines in doxorubicin[91], that prevent deep tumor penetration. In the case of PLX, the targets are TAMs in the TME (CSF-1R), and it will thus need to overcome all those barriers to exert their action upon pulmonary administration.

TAMs are highly abundant in the TME of BCLM and vastly contribute to tumor immunosuppression[62]. Oral administration (p.o.) of the CSF-1Ri PLX, in combination with standard of care chemotherapy, was shown to blunt the tumorigenic effect of TAMs, as shown by a reduction in lung metastases in a preclinical murine model of BC[40]. The abundance of immune infiltrates in the metastatic lung tumors was not assessed, however, in that study, and neither the effect of PLX p.o. alone in the lung metastases/burden. Clinically, p.o. administered PLX has been associated with hepatotoxicity, most likely because of the systemic exposure[49–51]. Such effects may limit the translation of such immunomodulators for use in combination with first line therapies in the treatment of BC and BC pulmonary metastases, as first line treatments have significant associated toxicity on their own[9–11].

PLX p.a. treatment was not expected to induce overt toxicity since the dose used in this study was low (1 mg/kg), as compared to the oral doses used in preclinical murine studies (40–800 mg/kg/day)[40–43,92–95]. Moreover, as opposed to delivery through the oral route, the fraction of drug that gets in contact with the liver upon pulmonary administration is expected to be relatively small[96]. Although PLX p.a. was well tolerated with no obvious overt toxicity to the animals either when administered alone or in combination with chemotherapy, the safety assessment in this work represents the first steps to a more detailed assessment of the toxicity of treatment and comparison with systemic administration of PLX, which may include assessment of lung, liver, and other tissues toxicities by clinical scoring using H&E staining, as well as evaluation of liver function by measuring liver enzymes and bilirubin levels.

There are several approaches that can be utilized to modulate TAMs in the TME. Those either promote the antitumor activity or reduce the tumorigenic function of TAMs. An example of inducing tumoricidal response is by interfering with markers on cancer cells. For instance, CD47 is expressed by tumor cells and through its interaction with SIRPα, prevents cancer cells from being phagocytosed by macrophages[23]. It has been shown that this access can be targeted by anti CD47 mABs, leading to activation of macrophage-mediated antibody-dependent cellular phagocytosis (ADCP)[97]. The tumor-promoting functions of TAMs can be reduced by several mechanisms. Recruitment of TAMs can be inhibited by

targeting the TAM-attracting chemokines CCL5 or CCL2, or their receptors. Another possible strategy is to use ICI therapies to interfere with the co-inhibitory molecules, PD-L1 and PD-L2, which are highly expressed on M2 TAMs and contribute to immunosuppressive functions[23]. Moreover, caspase-dependent apoptosis can be triggered in monocytes and macrophages using the anticancer trabectedin.

M2 TAMs can be selectively targeted based on their specific markers. An example of such study includes the use of peptides to precisely target M2 TAMs via interaction with CD206[98]. In our study we sought to inhibit CSF-1R, which it has been shown to result in a decrease in recruitment, survival and/or differentiation of infiltrates towards the M2-like TAM phenotype[37]. To enhance selectivity, it is possible to dual target TAMs via bispecific ligands[99], one promotes interaction with TAMs, such as peptide binding to CD206, and other binds to CSF-1R and inhibits its activation, such as PLX.

M2-like TAMs highly express CSF-1R, and their differentiation is largely dependent on CSF-1/CSF-1R signaling[22,38,39]. M2 phenotype polarization and proliferation is also mediated, at least in part, by activation of this axis[37,63,100,101]. The western blot and IF results shown here indirectly suggest that upon p.a. PLX (i) overcomes the extracellular lung barriers discussed above; (ii) permeates into the lung TME; finally (iii) reaching its cellular (macrophage) and intracellular molecular target (the CSF-1R).

Small molecules targeting the intracellular CSF-1R domain, including PLX, have also been shown to lead to an increase in M1/M2 ratio[94,102], which in turn correlates with improved therapeutic outcomes, including improving overall survival[42,44,45], increasing tumor infiltration of CD8+ cytotoxic T cells, and enhancing responses to chemotherapy and radiotherapy for patients with certain types of cancers, including pancreatic, ovarian and lung[42,44,45,103,104]. This alteration in the M1/M2 ratio may result from shifting the macrophages balance towards the anti-tumorigenic M1 TAM subset[94,] or overall more preferential decrease in the density of M2 compared to M1 TAMs[41]. However, the precise mechanism of repolarization/enrichment of a particular TAM phenotype is not entirely known but could be due to an increase in the release of cytokines that promote polarization of M1 TAMs, such as IFNγ and GM-CSF in response to CSF-1R inhibition[102]. In this work, an increase in M1/M2 ratio correlates with a decrease in burden of the secondary lung lesions[42].

Others have shown that systemic PLX administration prevents recruitment of TAMs into primary breast tumors[40] and TGCTs[27]. Our results show that the effect of PLX on lung metastatic lesions is different. In BCLM PLX leads to similar density of total (F4/80) TAMs, which show a shift towards a more classically activated phenotype (CD80, MHCII), consistent with an anti-tumorigenic effect. We interpret this result as a direct effect of the p.a. of the CSF-1R inhibitor, as its primary effect upon p.a. is in the population TAMs that have already been recruited to the lung TME. This is consistent with the fact that CSF-1Ri in gliomas and hepatocellular carcinoma[94,102] also results in reprogramming of the tissue-specific macrophage population.

The results reported here with PTX are important in many ways. PTX is first line therapy in patients with breast cancer and critical in the management of distant metastases[14]. It is also important to address the tolerability of the combination therapy. In stage IV TNBC, cancers spread to lungs, bone, brain, and liver[7]. Thus, in the clinic, systemic chemotherapy is needed for treatment of the primary and the metastatic cancers. It has been shown that CSF-1R inhibition by small molecules lead to increase in the response to standard of care therapy[40,93]. Therefore, the effect of chemotherapy on lung tumors could be enhanced by PLX. Further experimentation might reveal improved strategies regarding dosing regimens for both PTX and PLX in the combination therapy.

5. CONCLUSIONS

In this work we showed that upon local pulmonary administration in a BCLM model, PLX can overcome lung and tumor physiological barriers to reach and significantly inhibit its intracellular molecular target (CSF-1R), which is predominantly expressed in TAMs infiltrated in the TME. PLX as monotherapy and in combination with chemotherapy markedly reduced the number of M2-like TAMs and switched TAM polarization towards the M1 phenotype, resulting in an enhancement of M1/M2 ratio. These results correlate with an additive reduction in lung tumor burden when PLX is combined with i.v. administered PTX, as revealed by BLI and lung weight. The concentration of PLX used in this study was below the maximum tolerated dose (MTD) and without optimization of dosing schedule, thus leaving room for further improvement in antitumor efficacy. Locally administered TAM immunotherapy to the lungs may represent a safe and efficacious combination therapy to support first line chemotherapy in the treatment of BCLM and sets the stage for not only management of other secondary lung tumors, but also for treatment of primary lung cancers. Such an approach may be further enhanced as oral inhalation formulations of CSF-1Ris are developed for efficient outpatient treatment.

Supplementary Material

Refer to Web version on PubMed Central for supplementary material.

ACKNOWLEDGMENTS

We acknowledge partial financial support from the Center for Pharmaceutical Engineering and Sciences - School of Pharmacy at Virginia Commonwealth University (VCU) and National Science Foundation (DRM #1508363). Services and products in support of the research project were generated by the Virginia Commonwealth University Cancer Mouse Models Core Laboratory and Microscopy Facility supported, in part, with funding from NIH-NCI Cancer Center Support Grant P30 CA016059. SA, RA and FS acknowledge scholarships from King Saud and King Faisal Universities, and the Saudi Arabian Ministry of Education. The Authors also would like to thank the Flow Cytometry Shared Resource Core at VCU for help in cell sorting, and Dr. McClay, Department of Pharmacotherapy and Outcomes Science, School of Pharmacy at VCU for access to Western Blotting equipment.

6. REFERENCES

(1). Chambers AF; Groom AC; MacDonald IC Dissemination and Growth of Cancer Cells in Metastatic Sites. Nat Rev Cancer 2002, 2 (8), 563–572. 10.1038/nrc865. [PubMed: 12154349]

(2). Seyfried TN; Huysentruyt LC On the Origin of Cancer Metastasis. Crit Rev Oncog 2013, 18 (1–2), 43–73. [PubMed: 23237552]

(3). Stella GM; Kolling S; Benvenuti S; Bortolotto C Lung-Seeking Metastases. Cancers (Basel) 2019, 11 (7). 10.3390/cancers11071010.

(4). Kager L; Zoubek A; Pötschger U; Kastner U; Flege S; Kempf-Bielack B; Branscheid D; Kotz R; Salzer-Kuntschik M; Winkelmann W; Jundt G; Kabisch H; Reichardt P; Jürgens H; Gadner H; Bielack SS; Cooperative German-Austrian-Swiss Osteosarcoma Study Group. Primary Metastatic Osteosarcoma: Presentation and Outcome of Patients Treated on Neoadjuvant Cooperative Osteosarcoma Study Group Protocols. J. Clin. Oncol 2003, 21 (10), 2011–2018. 10.1200/JCO.2003.08.132. [PubMed: 12743156]

(5). Dan Z; Cao H; He X; Zhang Z; Zou L; Zeng L; Xu Y; Yin Q; Xu M; Zhong D; Yu H; Shen Q; Zhang P; Li Y A PH-Responsive Host-Guest Nanosystem Loading Succinobucol Suppresses Lung Metastasis of Breast Cancer. Theranostics 2016, 6 (3), 435–445. 10.7150/thno.13896. [PubMed: 26909117]

(6). Foulkes WD; Smith IE; Reis-Filho JS Triple-Negative Breast Cancer. N. Engl. J. Med 2010, 363 (20), 1938–1948. 10.1056/NEJMra1001389. [PubMed: 21067385]

(7). Xiao W; Zheng S; Liu P; Zou Y; Xie X; Yu P; Tang H; Xie X Risk Factors and Survival Outcomes in Patients with Breast Cancer and Lung Metastasis: A Population-Based Study. Cancer Med 2018, 7 (3), 922–930. 10.1002/cam4.1370. [PubMed: 29473333]

(8). Schmid P; Rugo HS; Adams S; Schneeweiss A; Barrios CH; Iwata H; Diéras V; Henschel V; Molinero L; Chui SY; Maiya V; Husain A; Winer EP; Loi S; Emens LA Atezolizumab plus Nab-Paclitaxel as First-Line Treatment for Unresectable, Locally Advanced or Metastatic Triple-Negative Breast Cancer (IMpassion130): Updated Efficacy Results from a Randomised, Double-Blind, Placebo-Controlled, Phase 3 Trial. The Lancet Oncology 2020, 21 (1), 44–59. 10.1016/S1470-2045(19)30689-8. [PubMed: 31786121]

(9). Weng X; Huang X; Li H; Lin S; Rao X; Guo X; Huang P First-Line Treatment With Atezolizumab Plus Nab-Paclitaxel for Advanced Triple-Negative Breast Cancer: A Cost-Effectiveness Analysis. American Journal of Clinical Oncology 2020, 43 (5), 340–348. 10.1097/COC.0000000000000671. [PubMed: 32028340]

(10). Kang C; Syed YY Atezolizumab (in Combination with Nab-Paclitaxel): A Review in Advanced Triple-Negative Breast Cancer. Drugs 2020, 80 (6), 601–607. 10.1007/s40265-020-01295-y. [PubMed: 32248356]

(11). Adams S; Loi S; Toppmeyer D; Cescon DW; De Laurentiis M; Nanda R; Winer EP; Mukai H; Tamura K; Armstrong A; Liu MC; Iwata H; Ryvo L; Wimberger P; Rugo HS; Tan AR; Jia L; Ding Y; Karantza V; Schmid P Pembrolizumab Monotherapy for Previously Untreated, PD-L1-Positive, Metastatic Triple-Negative Breast Cancer: Cohort B of the Phase II KEYNOTE-086 Study. Annals of Oncology 2019, 30 (3), 405–411. 10.1093/annonc/mdy518. [PubMed: 30475947]

(12). Zhang T; Prasad P; Cai P; He C; Shan D; Rauth AM; Wu XY Dual-Targeted Hybrid Nanoparticles of Synergistic Drugs for Treating Lung Metastases of Triple Negative Breast Cancer in Mice. Acta Pharmacol Sin 2017, 38 (6), 835–847. 10.1038/aps.2016.166. [PubMed: 28216624]

(13). Al-Mahmood S; Sapiezynski J; Garbuzenko OB; Minko T Metastatic and Triple-Negative Breast Cancer: Challenges and Treatment Options. Drug Deliv. and Transl. Res 2018, 8 (5), 1483–1507. 10.1007/s13346-018-0551-3. [PubMed: 29978332]

(14). Schmid P; Adams S; Rugo HS; Schneeweiss A; Barrios CH; Iwata H; Diéras V; Hegg R; Im S-A; Shaw Wright G; Henschel V; Molinero L; Chui SY; Funke R; Husain A; Winer EP; Loi S; Emens LA Atezolizumab and Nab-Paclitaxel in Advanced Triple-Negative Breast Cancer. New England Journal of Medicine 2018, 379 (22), 2108–2121. 10.1056/NEJMoa1809615.

(15). Schmid P; Cortes J; Pusztai L; McArthur H; Kümmel S; Bergh J; Denkert C; Park YH; Hui R; Harbeck N; Takahashi M; Foukakis T; Fasching PA; Cardoso F; Untch M; Jia L; Karantza V; Zhao J; Aktan G; Dent R; O'Shaughnessy J Pembrolizumab for Early Triple-Negative Breast Cancer. N Engl J Med 2020, 382 (9), 810–821. 10.1056/NEJMoa1910549. [PubMed: 32101663]

(16). Zou W; Wolchok JD; Chen L PD-L1 (B7-H1) and PD-1 Pathway Blockade for Cancer Therapy: Mechanisms, Response Biomarkers and Combinations. Sci Transl Med 2016, 8 (328), 328rv4. 10.1126/scitranslmed.aad7118.

(17). Akinleye A; Rasool Z Immune Checkpoint Inhibitors of PD-L1 as Cancer Therapeutics. J Hematol Oncol 2019, 12 (1), 92. 10.1186/s13045-019-0779-5. [PubMed: 31488176]

(18). Villadolid J; Amin A Immune Checkpoint Inhibitors in Clinical Practice: Update on Management of Immune-Related Toxicities. Transl Lung Cancer Res 2015, 4 (5), 560–575. 10.3978/j.issn.2218-6751.2015.06.06. [PubMed: 26629425]

(19). Fares CM; Van Allen EM; Drake CG; Allison JP; Hu-Lieskovan S Mechanisms of Resistance to Immune Checkpoint Blockade: Why Does Checkpoint Inhibitor Immunotherapy Not Work for All Patients? American Society of Clinical Oncology Educational Book 2019, No. 39, 147–164. 10.1200/EDBK_240837. [PubMed: 31099674]

(20). Nowicki TS; Hu-Lieskovan S; Ribas A Mechanisms of Resistance to PD-1 and PD-L1 Blockade: The Cancer Journal 2018, 24 (1), 47–53. 10.1097/PPO.0000000000000303. [PubMed: 29360728]

(21). Research, C. for D. E. and. FDA Issues Alert about Efficacy and Potential Safety Concerns with Atezolizumab in Combination with Paclitaxel for Treatment of Breast Cancer. FDA 2020.

(22). Cannarile MA; Weisser M; Jacob W; Jegg A-M; Ries CH; Rüttinger D Colony-Stimulating Factor 1 Receptor (CSF1R) Inhibitors in Cancer Therapy. J Immunother Cancer 2017, 5. 10.1186/s40425-017-0257-y.

(23). Mantovani A; Marchesi F; Malesci A; Laghi L; Allavena P Tumor-Associated Macrophages as Treatment Targets in Oncology. Nat Rev Clin Oncol 2017, 14 (7), 399–416. 10.1038/nrclinonc.2016.217. [PubMed: 28117416]

(24). Brown JM; Recht L; Strober S The Promise of Targeting Macrophages in Cancer Therapy. Clin Cancer Res 2017, 23 (13), 3241–3250. 10.1158/1078-0432.CCR-16-3122. [PubMed: 28341752]

(25). Lamb YN Pexidartinib: First Approval. Drugs 2019, 79 (16), 1805–1812. 10.1007/s40265-019-01210-0. [PubMed: 31602563]

(26). Lee J-H; Chen TW-W; Hsu C-H; Yen Y-H; Yang JC-H; Cheng A-L; Sasaki S; Chiu L. (Lillian); Sugihara M; Ishizuka T; Oguma T; Tajima N; Lin C-C A Phase I Study of Pexidartinib, a Colony-Stimulating Factor 1 Receptor Inhibitor, in Asian Patients with Advanced Solid Tumors. Invest New Drugs 2020, 38 (1), 99–110. 10.1007/s10637-019-00745-z. [PubMed: 30825104]

(27). Tap WD; Wainberg ZA; Anthony SP; Ibrahim PN; Zhang C; Healey JH; Chmielowski B; Staddon AP; Cohn AL; Shapiro GI; Keedy VL; Singh AS; Puzanov I; Kwak EL; Wagner AJ; Von Hoff DD; Weiss GJ; Ramanathan RK; Zhang J; Habets G; Zhang Y; Burton EA; Visor G; Sanftner L; Severson P; Nguyen H; Kim MJ; Marimuthu A; Tsang G; Shellooe R; Gee C; West BL; Hirth P; Nolop K; van de Rijn M; Hsu HH; Peterfy C; Lin PS; Tong-Starksen S; Bollag G Structure-Guided Blockade of CSF1R Kinase in Tenosynovial Giant-Cell Tumor. N. Engl. J. Med 2015, 373 (5), 428–437. 10.1056/NEJMoa1411366. [PubMed: 26222558]

(28). Clinicaltrials.gov. https://clinicaltrials.gov/ct2/show/NCT01042379?term=NCT01042379&draw=2&rank=1(Accessed October 22, 2020), Neoadjuvant and Personalized Adaptive Novel Agents to Treat Breast Cancer (I-SPY).

(29). Wojtkowiak JW; Verduzco D; Schramm KJ; Gillies RJ Drug Resistance and Cellular Adaptation to Tumor Acidic PH Microenvironment. Mol. Pharmaceutics 2011, 8 (6), 2032–2038. 10.1021/mp200292c.

(30). Balkwill FR; Capasso M; Hagemann T The Tumor Microenvironment at a Glance. J. Cell. Sci 2012, 125 (Pt 23), 5591–5596. 10.1242/jcs.116392. [PubMed: 23420197]

(31). Zang X; Zhang X; Hu H; Qiao M; Zhao X; Deng Y; Chen D Targeted Delivery of Zoledronate to Tumor-Associated Macrophages for Cancer Immunotherapy. Mol. Pharm 2019, 16 (5), 2249–2258. 10.1021/acs.molpharmaceut.9b00261. [PubMed: 30969779]

(32). Slaney CY; Kershaw MH; Darcy PK Trafficking of T Cells into Tumors. Cancer Res. 2014, 74 (24), 7168–7174. 10.1158/0008-5472.CAN-14-2458. [PubMed: 25477332]

(33). Deci MB; Ferguson SW; Scatigno SL; Nguyen J Modulating Macrophage Polarization through CCR2 Inhibition and Multivalent Engagement. Mol. Pharmaceutics 2018, 15 (7), 2721–2731. 10.1021/acs.molpharmaceut.8b00237.

(34). Grivennikov SI; Greten FR; Karin M Immunity, Inflammation, and Cancer. Cell 2010, 140 (6), 883–899. 10.1016/j.cell.2010.01.025. [PubMed: 20303878]

(35). Italiani P; Boraschi D From Monocytes to M1/M2 Macrophages: Phenotypical vs. Functional Differentiation. Front Immunol 2014, 5, 514. 10.3389/fimmu.2014.00514. [PubMed: 25368618]

(36). Zhu S; Niu M; O'Mary H; Cui Z Targeting of Tumor-Associated Macrophages Made Possible by PEG-Sheddable, Mannose-Modified Nanoparticles. Mol. Pharmaceutics 2013, 10 (9), 3525–3530. 10.1021/mp400216r.

(37). Laoui D; Van Overmeire E; De Baetselier P; Van Ginderachter JA; Raes G Functional Relationship between Tumor-Associated Macrophages and Macrophage Colony-Stimulating Factor as Contributors to Cancer Progression. Front Immunol 2014, 5, 489. 10.3389/fimmu.2014.00489. [PubMed: 25339957]

(38). Rovida E; Sbarba PD Colony-Stimulating Factor-1 Receptor in the Polarization of Macrophages: A Target for Turning Bad to Good Ones? J Clin Cell Immunol 2015, 06 (06). 10.4172/2155-9899.1000379.

(39). Fleetwood AJ; Lawrence T; Hamilton JA; Cook AD Granulocyte-Macrophage Colony-Stimulating Factor (CSF) and Macrophage CSF-Dependent Macrophage Phenotypes Display Differences in Cytokine Profiles and Transcription Factor Activities: Implications for CSF Blockade in Inflammation. J. Immunol 2007, 178 (8), 5245–5252. 10.4049/jimmunol.178.8.5245. [PubMed: 17404308]

(40). DeNardo DG; Brennan DJ; Rexhepaj E; Ruffell B; Shiao SL; Madden SF; Gallagher WM; Wadhwani N; Keil SD; Junaid SA; Rugo HS; Hwang ES; Jirström K; West BL; Coussens LM Leukocyte Complexity Predicts Breast Cancer Survival and Functionally Regulates Response to Chemotherapy. Cancer Discov 2011, 1, 54–67. 10.1158/2159-8274.CD-10-0028. [PubMed: 22039576]

(41). Yan D; Kowal J; Akkari L; Schuhmacher AJ; Huse JT; West BL; Joyce JA Inhibition of Colony Stimulating Factor-1 Receptor Abrogates Microenvironment-Mediated Therapeutic Resistance in Gliomas. Oncogene 2017, 36 (43), 6049–6058. 10.1038/onc.2017.261. [PubMed: 28759044]

(42). Zhu Y; Knolhoff BL; Meyer MA; Nywening TM; West BL; Luo J; Wang-Gillam A; Goedegebuure SP; Linehan DC; DeNardo DG CSF1/CSF1R Blockade Reprograms Tumor-Infiltrating Macrophages and Improves Response to T-Cell Checkpoint Immunotherapy in Pancreatic Cancer Models. Cancer Res. 2014, 74 (18), 5057–5069. 10.1158/0008-5472.CAN-13-3723. [PubMed: 25082815]

(43). Mok S; Koya RC; Tsui C; Xu J; Robert L; Wu L; Graeber T; West BL; Bollag G; Ribas A Inhibition of CSF-1 Receptor Improves the Antitumor Efficacy of Adoptive Cell Transfer Immunotherapy. Cancer Res. 2014, 74 (1), 153–161. 10.1158/0008-5472.CAN-13-1816. [PubMed: 24247719]

(44). Ma J; Liu L; Che G; Yu N; Dai F; You Z The M1 Form of Tumor-Associated Macrophages in Non-Small Cell Lung Cancer Is Positively Associated with Survival Time. BMC Cancer 2010, 10, 112. 10.1186/1471-2407-10-112. [PubMed: 20338029]

(45). Cm O; A S; Rh G; Da W; P B Macrophages within NSCLC Tumour Islets Are Predominantly of a Cytotoxic M1 Phenotype Associated with Extended Survival. Eur Respir J 2009, 33 (1), 118–126. 10.1183/09031936.00065708. [PubMed: 19118225]

(46). Zhang Y; Cheng S; Zhang M; Zhen L; Pang D; Zhang Q; Li Z High-Infiltration of Tumor-Associated Macrophages Predicts Unfavorable Clinical Outcome for Node-Negative Breast Cancer. PLoS ONE 2013, 8 (9), e76147. 10.1371/journal.pone.0076147. [PubMed: 24098773]

(47). A Study of PLX3397 in Patients With Unresectable or Metastatic KIT-mutated Melanoma - Full Text View - ClinicalTrials.gov https://clinicaltrials.gov/ct2/show/NCT02975700 (accessed Jun 25, 2020).

(48). West RB; Rubin BP; Miller MA; Subramanian S; Kaygusuz G; Montgomery K; Zhu S; Marinelli RJ; De Luca A; Downs-Kelly E; Goldblum JR; Corless CL; Brown PO; Gilks CB; Nielsen TO; Huntsman D; van de Rijn M A Landscape Effect in Tenosynovial Giant-Cell Tumor from Activation of CSF1 Expression by a Translocation in a Minority of Tumor Cells. Proc Natl Acad Sci U S A 2006, 103 (3), 690–695. 10.1073/pnas.0507321103. [PubMed: 16407111]

(49). Wesolowski R; Sharma N; Reebel L; Rodal MB; Peck A; West BL; Marimuthu A; Severson P; Karlin DA; Dowlati A; Le MH; Coussens LM; Rugo HS Phase Ib Study of the Combination of Pexidartinib (PLX3397), a CSF-1R Inhibitor, and Paclitaxel in Patients with Advanced Solid Tumors. Ther Adv Med Oncol 2019, 11, 1758835919854238. 10.1177/1758835919854238.

(50). Tap WD; Gelderblom H; Palmerini E; Desai J; Bauer S; Blay J-Y; Alcindor T; Ganjoo K; Martín-Broto J; Ryan CW; Thomas DM; Peterfy C; Healey JH; Sande M. van de; Gelhorn HL; Shuster DE; Wang Q; Yver A; Hsu HH; Lin PS; Tong-Starksen S; Stacchiotti S; Wagner AJ Pexidartinib versus Placebo for Advanced Tenosynovial Giant Cell Tumour (ENLIVEN): A Randomised Phase 3 Trial. The Lancet 2019, 394 (10197), 478–487. 10.1016/S0140-6736(19)30764-0.

(51). Piawah S; Hyland C; Umetsu SE; Esserman LJ; Rugo HS; Chien AJ A Case Report of Vanishing Bile Duct Syndrome after Exposure to Pexidartinib (PLX3397) and Paclitaxel. NPJ Breast Cancer 2019, 5, 17. 10.1038/s41523-019-0112-z. [PubMed: 31240240]

(52). Posch C; Weihsengruber F; Bartsch K; Feichtenschlager V; Sanlorenzo M; Vujic I; Monshi B; Ortiz-Urda S; Rappersberger K Low-Dose Inhalation of Interleukin-2 Bio-Chemotherapy for the Treatment of Pulmonary Metastases in Melanoma Patients. Br. J. Cancer 2014, 110 (6), 1427–1432. 10.1038/bjc.2014.62. [PubMed: 24518593]

(53). Biot C; Rentsch CA; Gsponer JR; Birkhäuser FD; Jusforgues-Saklani H; Lemaître F; Auriau C; Bachmann A; Bousso P; Demangel C; Peduto L; Thalmann GN; Albert ML Preexisting BCG-Specific T Cells Improve Intravesical Immunotherapy for Bladder Cancer. Sci Transl Med 2012, 4 (137), 137ra72. 10.1126/scitranslmed.3003586.

(54). Milling L; Zhang Y; Irvine DJ Delivering Safer Immunotherapies for Cancer. Adv Drug Deliv Rev 2017, 114, 79–101. 10.1016/j.addr.2017.05.011. [PubMed: 28545888]

(55). Pawar A; Prabhu P Nanosoldiers: A Promising Strategy to Combat Triple Negative Breast Cancer. Biomedicine & Pharmacotherapy 2019, 110, 319–341. 10.1016/j.biopha.2018.11.122. [PubMed: 30529766]

(56). Chen C; Nong Z; Xie Q; He J; Cai W; Tang X; Chen X; Huang R; Gao Y 2-Dodecyl-6-Methoxycyclohexa-2,5-Diene-1,4-Dione Inhibits the Growth and Metastasis of Breast Carcinoma in Mice. Sci Rep 2017, 7 (1), 6704. 10.1038/s41598-017-07162-3. [PubMed: 28751740]

(57). Ghosh A; Sarkar S; Banerjee S; Behbod F; Tawfik O; McGregor D; Graff S; Banerjee SK MIND Model for Triple-Negative Breast Cancer in Syngeneic Mice for Quick and Sequential Progression Analysis of Lung Metastasis. PLoS ONE 2018, 13 (5), e0198143. 10.1371/journal.pone.0198143. [PubMed: 29813119]

(58). Steenbrugge J; Breyne K; Demeyere K; De Wever O; Sanders NN; Van Den Broeck W; Colpaert C; Vermeulen P; Van Laere S; Meyer E Anti-Inflammatory Signaling by Mammary Tumor Cells Mediates Prometastatic Macrophage Polarization in an Innovative Intraductal Mouse Model for Triple-Negative Breast Cancer. J Exp Clin Cancer Res 2018, 37 (1), 191. 10.1186/s13046-018-0860-x. [PubMed: 30111338]

(59). Hong H; Zhang Y; Severin GW; Yang Y; Engle JW; Niu G; Nickles RJ; Chen X; Leigh BR; Barnhart TE; Cai W Multimodality Imaging of Breast Cancer Experimental Lung Metastasis with Bioluminescence and a Monoclonal Antibody Dual-Labeled with 89Zr and IRDye 800CW. Mol. Pharm 2012, 9 (8), 2339–2349. 10.1021/mp300277f. [PubMed: 22784250]

(60). Li S; Xu X; Jiang M; Bi Y; Xu J; Han M Lipopolysaccharide Induces Inflammation and Facilitates Lung Metastasis in a Breast Cancer Model via the Prostaglandin E2-EP2 Pathway. Mol Med Rep 2015, 11 (6), 4454–4462. 10.3892/mmr.2015.3258. [PubMed: 25625500]

(61). Kampan NC; Madondo MT; McNally OM; Quinn M; Plebanski M Paclitaxel and Its Evolving Role in the Management of Ovarian Cancer https://www.hindawi.com/journals/bmri/2015/413076/ (accessed May 20, 2020). 10.1155/2015/413076.

(62). Argyle D; Kitamura T Targeting Macrophage-Recruiting Chemokines as a Novel Therapeutic Strategy to Prevent the Progression of Solid Tumors. Front. Immunol 2018, 9. 10.3389/fimmu.2018.02629.

(63). Achkova D; Maher J Role of the Colony-Stimulating Factor (CSF)/CSF-1 Receptor Axis in Cancer. Biochem. Soc. Trans 2016, 44 (2), 333–341. 10.1042/BST20150245. [PubMed: 27068937]

(64). Van Dalen FJ; Van Stevendaal MHME; Fennemann FL; Verdoes M; Ilina O Molecular Repolarisation of Tumour-Associated Macrophages. Molecules 2019, 24 (1), 9. 10.3390/molecules24010009.

(65). Muraoka D; Seo N; Hayashi T; Tahara Y; Fujii K; Tawara I; Miyahara Y; Okamori K; Yagita H; Imoto S; Yamaguchi R; Komura M; Miyano S; Goto M; Sawada S; Asai A; Ikeda H; Akiyoshi K;

Harada N; Shiku H Antigen Delivery Targeted to Tumor-Associated Macrophages Overcomes Tumor Immune Resistance. J Clin Invest 129 (3), 1278–1294. 10.1172/JCI97642.

(66). Larkin J; Chiarion-Sileni V; Gonzalez R; Grob J-J; Rutkowski P; Lao CD; Cowey CL; Schadendorf D; Wagstaff J; Dummer R; Ferrucci PF; Smylie M; Hogg D; Hill A; Márquez-Rodas I; Haanen J; Guidoboni M; Maio M; Schöffski P; Carlino MS; Lebbé C; McArthur G; Ascierto PA; Daniels GA; Long GV; Bastholt L; Rizzo JI; Balogh A; Moshyk A; Hodi FS; Wolchok JD Five-Year Survival with Combined Nivolumab and Ipilimumab in Advanced Melanoma. N Engl J Med 2019, 381 (16), 1535–1546. 10.1056/NEJMoa1910836. [PubMed: 31562797]

(67). Reck M; Rodríguez-Abreu D; Robinson AG; Hui R; Csőszi T; Fülöp A; Gottfried M; Peled N; Tafreshi A; Cuffe S; O'Brien M; Rao S; Hotta K; Leiby MA; Lubiniecki GM; Shentu Y; Rangwala R; Brahmer JR Pembrolizumab versus Chemotherapy for PD-L1–Positive Non–Small-Cell Lung Cancer. N Engl J Med 2016, 375 (19), 1823–1833. 10.1056/NEJMoa1606774. [PubMed: 27718847]

(68). Overman MJ; Lonardi S; Wong KYM; Lenz H-J; Gelsomino F; Aglietta M; Morse MA; Van Cutsem E; McDermott R; Hill A; Sawyer MB; Hendlisz A; Neyns B; Svrcek M; Moss RA; Ledeine J-M; Cao ZA; Kamble S; Kopetz S; André T Durable Clinical Benefit With Nivolumab Plus Ipilimumab in DNA Mismatch Repair–Deficient/Microsatellite Instability–High Metastatic Colorectal Cancer. JCO 2018, 36 (8), 773–779. 10.1200/JCO.2017.76.9901.

(69). Tarantino P; Morganti S; Curigliano G Biologic Therapy for Advanced Breast Cancer: Recent Advances and Future Directions. Expert Opinion on Biological Therapy 2020, 1–15. 10.1080/14712598.2020.1752176.

(70). Broderick SR Adjuvant and Neoadjuvant Immunotherapy in Non–Small Cell Lung Cancer. Thoracic Surgery Clinics 2020, 30 (2), 215–220. 10.1016/j.thorsurg.2020.01.001. [PubMed: 32327180]

(71). Ribas A; Wolchok JD Cancer Immunotherapy Using Checkpoint Blockade. Science 2018, 359 (6382), 1350–1355. 10.1126/science.aar4060. [PubMed: 29567705]

(72). Den Otter W; Jacobs JJL; Battermann JJ; Hordijk GJ; Krastev Z; Moiseeva EV; Stewart RJE; Ziekman PGPM; Koten JW Local Therapy of Cancer with Free IL-2. Cancer Immunol Immunother 2008, 57 (7), 931–950. 10.1007/s00262-008-0455-z. [PubMed: 18256831]

(73). Cheng C; Haouala A; Krueger T; Mithieux F; Perentes JY; Peters S; Decosterd LA; Ris H-B Drug Uptake in a Rodent Sarcoma Model after Intravenous Injection or Isolated Lung Perfusion of Free/Liposomal Doxorubicin. Interactive CardioVascular and Thoracic Surgery 2009, 8 (6), 635–638. 10.1510/icvts.2008.194720. [PubMed: 19282323]

(74). Guilleminault. The Airways: A Promising Route for the Pulmonary Delivery of Anticancer Agents. Advances in Cancer Therapy 2011. 10.5772/24910.

(75). Tseng C-L; Su W-Y; Yen K-C; Yang K-C; Lin F-H The Use of Biotinylated-EGF-Modified Gelatin Nanoparticle Carrier to Enhance Cisplatin Accumulation in Cancerous Lungs via Inhalation. Biomaterials 2009, 30 (20), 3476–3485. 10.1016/j.biomaterials.2009.03.010. [PubMed: 19345990]

(76). Selting K; Waldrep JC; Reinero C; Branson K; Gustafson D; Kim DY; Henry C; Owen N; Madsen R; Dhand R Feasibility and Safety of Targeted Cisplatin Delivery to a Select Lung Lobe in Dogs via the AeroProbe Intracorporeal Nebulization Catheter. J Aerosol Med Pulm Drug Deliv 2008, 21 (3), 255–268. 10.1089/jamp.2008.0684. [PubMed: 18759657]

(77). Otterson GA; Villalona-Calero MA; Sharma S; Kris MG; Imondi A; Gerber M; White DA; Ratain MJ; Schiller JH; Sandler A; Kraut M; Mani S; Murren JR Phase I Study of Inhaled Doxorubicin for Patients with Metastatic Tumors to the Lungs. Clinical Cancer Research 2007, 13 (4), 1246–1252. 10.1158/1078-0432.CCR-06-1096. [PubMed: 17317836]

(78). Huland E; Burger A; Fleischer J; Fornara P; Hatzmann E; Heidenreich A; Heinzer H; Heynemann H; Hoffmann L; Hofmann R; Huland H; Kämpfer I; Kindler M; Kirchner H; Mehlhorn G; Moniak TH; Rebmann U; Roigas J; Schneider TH; Schnorr D; Schmitz HJ; Wenisch R; Varga Z; Vinke J Efficacy and Safety of Inhaled Recombinant Interleukin-2 in High-Risk Renal Cell Cancer Patients Compared with Systemic Interleukin-2: An Outcome Study. Folia Biol. (Praha) 2003, 49 (5), 183–190. [PubMed: 14680292]

(79). Rosière R; Berghmans T; De Vuyst P; Amighi K; Wauthoz N The Position of Inhaled Chemotherapy in the Care of Patients with Lung Tumors: Clinical Feasibility and Indications According to Recent Pharmaceutical Progresses. Cancers 2019, 11 (3), 329. 10.3390/cancers11030329.

(80). Otterson GA; Villalona-Calero MA; Hicks W; Pan X; Ellerton JA; Gettinger SN; Murren JR Phase I/II Study of Inhaled Doxorubicin Combined with Platinum-Based Therapy for Advanced Non-Small Cell Lung Cancer. Clinical Cancer Research 2010, 16 (8), 2466–2473. 10.1158/1078-0432.CCR-09-3015. [PubMed: 20371682]

(81). Chou AJ; Gupta R; Bell MD; Riewe KO; Meyers PA; Gorlick R Inhaled Lipid Cisplatin (ILC) in the Treatment of Patients with Relapsed/Progressive Osteosarcoma Metastatic to the Lung. Pediatr Blood Cancer 2013, 60 (4), 580–586. 10.1002/pbc.24438. [PubMed: 23255417]

(82). Zarogoulidis P; Chatzaki E; Porpodis K; Domvri K; Hohenforst-Schmidt W; Goldberg EP; Karamanos N; Zarogoulidis K Inhaled Chemotherapy in Lung Cancer: Future Concept of Nanomedicine. Int J Nanomedicine 2012, 7, 1551–1572. 10.2147/IJN.S29997. [PubMed: 22619512]

(83). Verschraegen CF Clinical Evaluation of the Delivery and Safety of Aerosolized Liposomal 9-Nitro-20(S)-Camptothecin in Patients with Advanced Pulmonary Malignancies. Clinical Cancer Research 2004, 10 (7), 2319–2326. 10.1158/1078-0432.CCR-0929-3. [PubMed: 15073107]

(84). Rosenberg SA; Yannelli JR; Yang JC; Topalian SL; Schwartzentruber DJ; Weber JS; Parkinson DR; Seipp CA; Einhorn JH; White DE Treatment of Patients with Metastatic Melanoma with Autologous Tumor-Infiltrating Lymphocytes and Interleukin 2. J. Natl. Cancer Inst 1994, 86 (15), 1159–1166. 10.1093/jnci/86.15.1159. [PubMed: 8028037]

(85). Huland E; Heinzer H; Huland H Treatment of Pulmonary Metastatic Renal-Cell Carcinoma in 116 Patients Using Inhaled Interleukin-2 (IL-2). Anticancer Res. 1999, 19 (4A), 2679–2683. [PubMed: 10470219]

(86). Arndt CAS; Koshkina NV; Inwards CY; Hawkins DS; Krailo MD; Villaluna D; Anderson PM; Goorin AM; Blakely ML; Bernstein M; Bell SA; Ray K; Grendahl DC; Marina N; Kleinerman ES INHALED GM-CSF FOR FIRST PULMONARY RECURRENCE OF OSTEOSARCOMA; EFFECTS ON DISEASE FREE SURVIVAL AND IMMUNOMODULATION: A REPORT FROM THE CHILDREN'S ONCOLOGY GROUP. Clin Cancer Res 2010, 16 (15), 4024–4030. 10.1158/1078-0432.CCR-10-0662. [PubMed: 20576718]

(87). Ghadiri M; Young PM; Traini D Strategies to Enhance Drug Absorption via Nasal and Pulmonary Routes. Pharmaceutics 2019, 11 (3). 10.3390/pharmaceutics11030113.

(88). Mangal S; Gao W; Li T; Zhou Q. (Tony). Pulmonary Delivery of Nanoparticle Chemotherapy for the Treatment of Lung Cancers: Challenges and Opportunities. Acta Pharmacol Sin 2017, 38 (6), 782–797. 10.1038/aps.2017.34. [PubMed: 28504252]

(89). Ruge CA; Schaefer UF; Herrmann J; Kirch J; Cañadas O; Echaide M; Pérez-Gil J; Casals C; Müller R; Lehr C-M The Interplay of Lung Surfactant Proteins and Lipids Assimilates the Macrophage Clearance of Nanoparticles. PLoS ONE 2012, 7 (7), e40775. 10.1371/journal.pone.0040775. [PubMed: 22802970]

(90). Patel K; Doddapaneni R; Sekar V; Chowdhury N; Singh M Combination Approach of YSA Peptide Anchored Docetaxel Stealth Liposomes with Oral Antifibrotic Agent for the Treatment of Lung Cancer. Mol. Pharmaceutics 2016, 13 (6), 2049–2058. 10.1021/acs.molpharmaceut.6b00187.

(91). Almuqbil RM; Heyder RS; Bielski ER; Durymanov M; Reineke JJ; da Rocha SRP Dendrimer Conjugation Enhances Tumor Penetration and Efficacy of Doxorubicin in Extracellular Matrix-Expressing 3D Lung Cancer Models. Mol. Pharmaceutics 2020, 17 (5), 1648–1662. 10.1021/acs.molpharmaceut.0c00083.

(92). Peranzoni E; Lemoine J; Vimeux L; Feuillet V; Barrin S; Kantari-Mimoun C; Bercovici N; Guérin M; Biton J; Ouakrim H; Régnier F; Lupo A; Alifano M; Damotte D; Donnadieu E Macrophages Impede CD8 T Cells from Reaching Tumor Cells and Limit the Efficacy of Anti–PD-1 Treatment. PNAS 2018, 115 (17), E4041–E4050. 10.1073/pnas.1720948115. [PubMed: 29632196]

(93). Mitchem JB; Brennan DJ; Knolhoff BL; Belt BA; Zhu Y; Sanford DE; Belaygorod L; Carpenter D; Collins L; Piwnica-Worms D; Hewitt S; Udupi GM; Gallagher WM; Wegner C; West BL;

Wang-Gillam A; Goedegebuure SP; Linehan DC; DeNardo DG Targeting Tumor-Infiltrating Macrophages Decreases Tumor-Initiating Cells, Relieves Immunosuppression and Improves Chemotherapeutic Responses. Cancer Res 2013, 73 (3), 1128–1141. 10.1158/0008-5472.CAN-12-2731. [PubMed: 23221383]

(94). Ao J-Y; Zhu X-D; Chai Z-T; Cai H; Zhang Y-Y; Zhang K-Z; Kong L-Q; Zhang N; Ye B-G; Ma D-N; Sun H-C Colony-Stimulating Factor 1 Receptor Blockade Inhibits Tumor Growth by Altering the Polarization of Tumor-Associated Macrophages in Hepatocellular Carcinoma. Mol. Cancer Ther 2017, 16 (8), 1544–1554. 10.1158/1535-7163.MCT-16-0866. [PubMed: 28572167]

(95). Shiao SL; B R; Dg D; Ba F; Cc P; Lm C TH2-Polarized CD4(+) T Cells and Macrophages Limit Efficacy of Radiotherapy https://pubmed.ncbi.nlm.nih.gov/25716473/ (accessed Oct 14, 2020). 10.1158/2326-6066.CIR-14-0232.

(96). Kumar Verma R; Mukker JK; Singh RSP; Kumar K; Verma PRP; Misra A Partial Biodistribution and Pharmacokinetics of Isoniazid and Rifabutin Following Pulmonary Delivery of Inhalable Microparticles to Rhesus Macaques. Mol. Pharm 2012, 9 (4), 1011–1016. 10.1021/mp300043f. [PubMed: 22397370]

(97). McCracken MN; Cha AC; Weissman IL Molecular Pathways: Activating T Cells after Cancer Cell Phagocytosis from Blockade of CD47 “Don’t Eat Me” Signals. Clin Cancer Res 2015, 21 (16), 3597–3601. 10.1158/1078-0432.CCR-14-2520. [PubMed: 26116271]

(98). Lepland A; Asciutto EK; Malfanti A; Simón-Gracia L; Sidorenko V; Vicent MJ; Teesalu T; Scodeller P Targeting Pro-Tumoral Macrophages in Early Primary and Metastatic Breast Tumors with the CD206-Binding MUNO Peptide. Mol. Pharmaceutics 2020, 17 (7), 2518–2531. 10.1021/acs.molpharmaceut.0c00226.

(99). Ngambenjawong C; Gustafson HH; Pun SH Progress in Tumor-Associated Macrophage (TAM)-Targeted Therapeutics. Adv Drug Deliv Rev 2017, 114, 206–221. 10.1016/j.addr.2017.04.010. [PubMed: 28449873]

(100). Holmgaard RB; Zamarin D; Lesokhin A; Merghoub T; Wolchok JD Targeting Myeloid-Derived Suppressor Cells with Colony Stimulating Factor-1 Receptor Blockade Can Reverse Immune Resistance to Immunotherapy in Indoleamine 2,3-Dioxygenase-Expressing Tumors. EBioMedicine 2016, 6, 50–58. 10.1016/j.ebiom.2016.02.024. [PubMed: 27211548]

(101). Genard G; Lucas S; Michiels C Reprogramming of Tumor-Associated Macrophages with Anticancer Therapies: Radiotherapy versus Chemo- and Immunotherapies. Front Immunol 2017, 8, 828. 10.3389/fimmu.2017.00828. [PubMed: 28769933]

(102). Pyonteck SM; Akkari L; Schuhmacher AJ; Bowman RL; Sevenich L; Quail DF; Olson OC; Quick ML; Huse JT; Teijeiro V; Setty M; Leslie CS; Oei Y; Pedraza A; Zhang J; Brennan CW; Sutton JC; Holland EC; Daniel D; Joyce JA CSF-1R Inhibition Alters Macrophage Polarization and Blocks Glioma Progression. Nat Med 2013, 19 (10), 1264–1272. 10.1038/nm.3337. [PubMed: 24056773]

(103). Zhang M; He Y; Sun X; Li Q; Wang W; Zhao A; Di W A High M1/M2 Ratio of Tumor-Associated Macrophages Is Associated with Extended Survival in Ovarian Cancer Patients. J Ovarian Res 2014, 7, 19. 10.1186/1757-2215-7-19. [PubMed: 24507759]

(104). Jayasingam SD; Citartan M; Thang TH; Mat Zin AA; Ang KC; Ch’ng ES Evaluating the Polarization of Tumor-Associated Macrophages Into M1 and M2 Phenotypes in Human Cancer Tissue: Technicalities and Challenges in Routine Clinical Practice. Front Oncol 2020, 9. 10.3389/fonc.2019.01512.

(A)

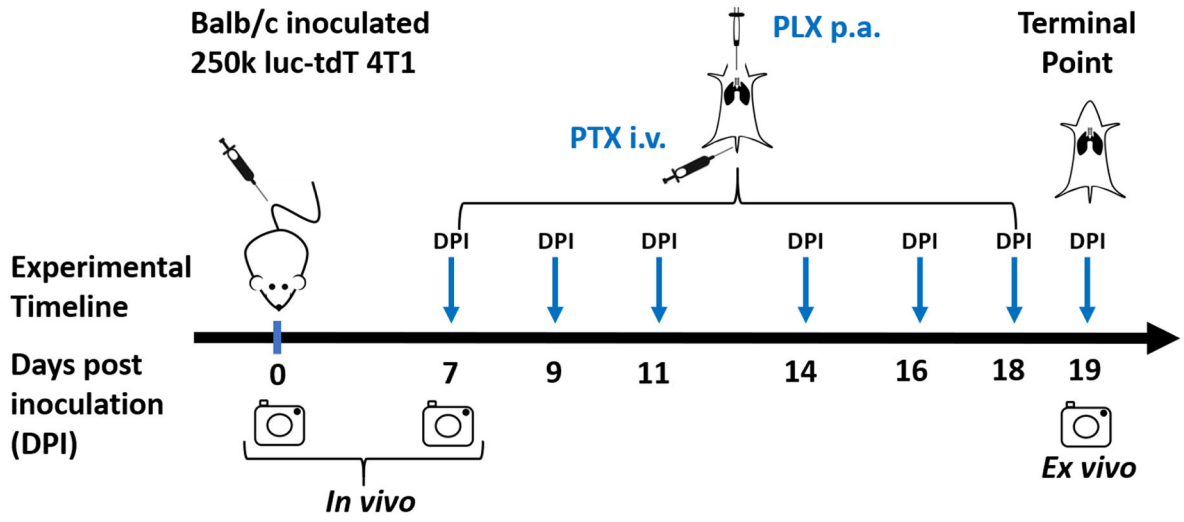

(B)

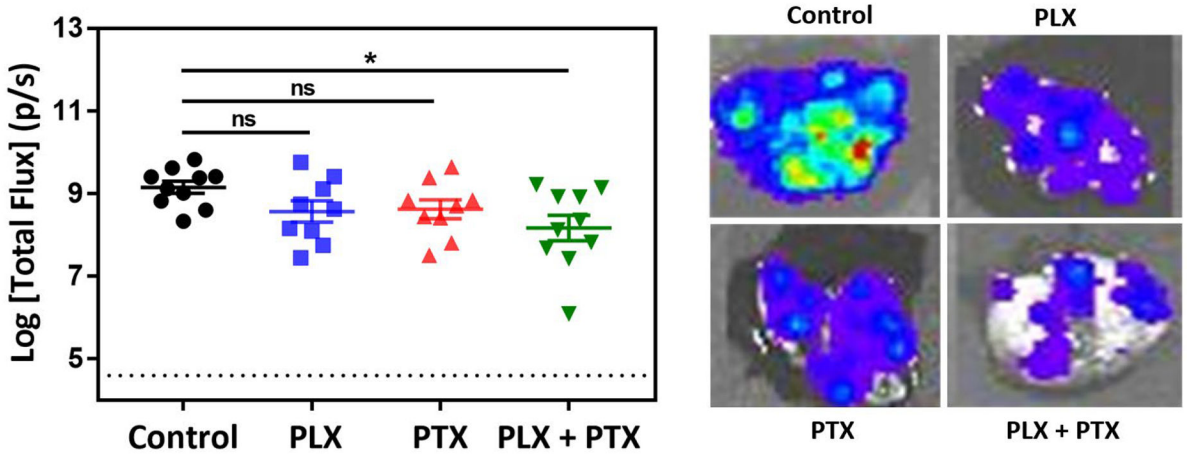

(C)

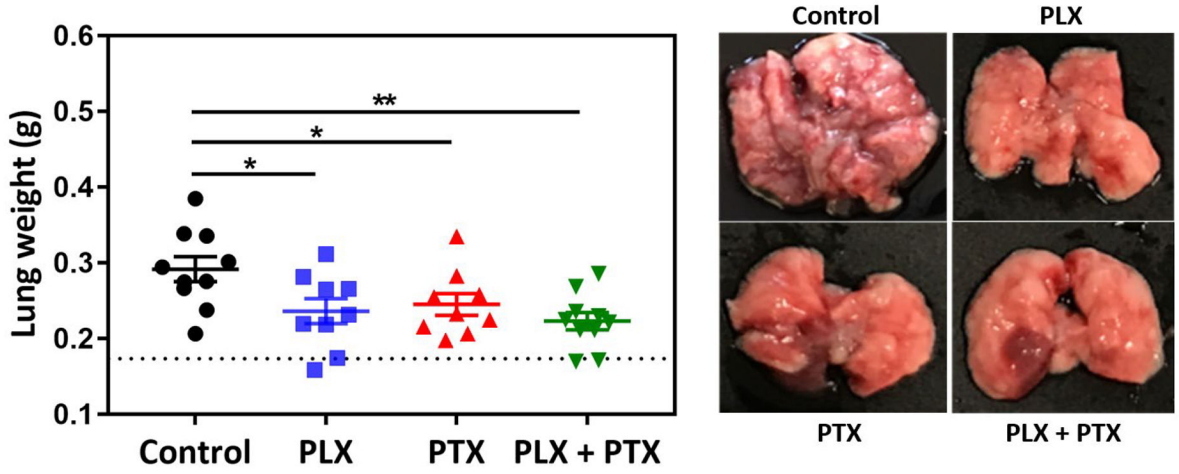

(D)

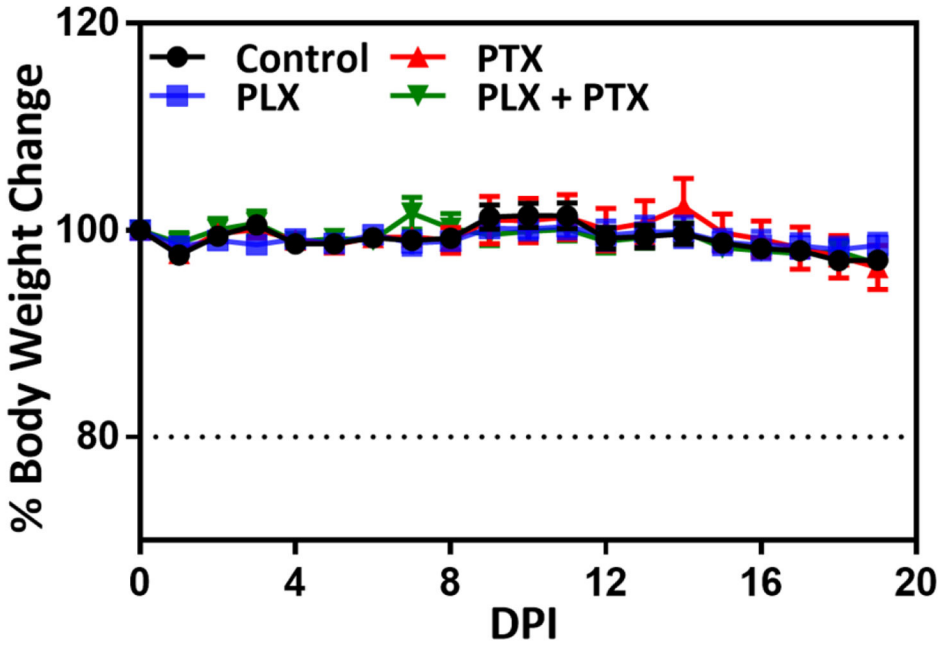

Figure 1.

Immunochemotherapy reduces tumor burden *in vivo*. **(A)** *Experimental timeline;* animals were randomized and allocated into groups on day 7 prior to treatment, arrows indicate treatment days with vehicle (1% DMSO, 5% tween80, PBS, p.a.), 1mg/kg PLX (p.a.), 1mg/kg PTX (i.v.), and 1 mg/kg PLX (p.a.) + 1 mg/kg PTX (i.v.) combination, experiment was terminated on day 19; **(B)** *ex vivo* bioluminescence analysis of tumor burden via *ex vivo* lung imaging on the terminal day, grid line indicates the baseline flux acquired by imaging of lungs of nontumor bearing animals (n=3); statistical significance was determined using Kruskal Wallis test (*p <0.05), data represented as mean ±SEM (n=9–10). **(C)** tumor burden assessed by lung weight on the terminal day, grid line indicates the average lung weight of nontumor bearing animals (n=3); statistical significance was determined using One-way ANOVA (*p <0.05, **p <0.01), data represented as mean ±SEM (n=9–10), **(D)** measurement of body weights represented by percentage changes from day zero (100%) to the terminal day.

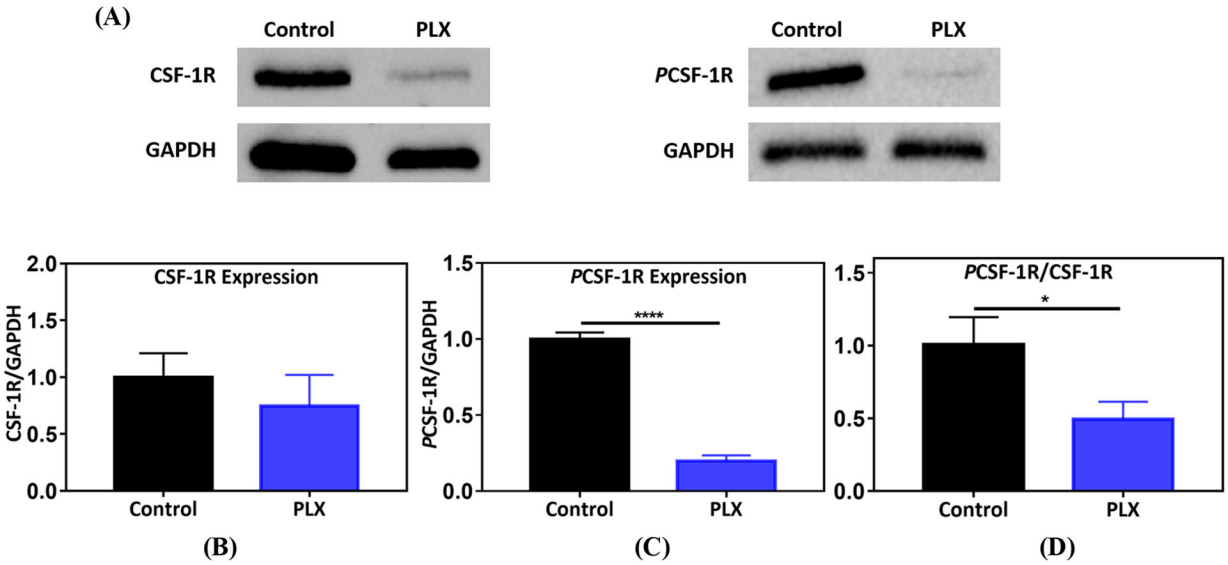

Figure 2.

Colony stimulating factor-1 receptor (CSF-1R) inhibition by PLX. **(A)** Protein bands for CSF-1R, *P*CSF-1R, and GAPDH, generated by western blot analysis on PLX (1 mg/kg, p.a.) treated lung tumor nodules, **(B)** effect of PLX on CSF-1R expression (n=7), **(C)** impact of treatment on *P*CSF-1R expression (n=7). For (B) and (C), protein densities were normalized to GAPDH, **(D)** ratio of *P*CSF-1R/CSF-1R. Control and PLX samples were normalized to average control in each independent experiment. Statistical significance was calculated by direct comparison using unpaired t test (*p <0.05,****p <0.0001), data represented as mean ±SEM.

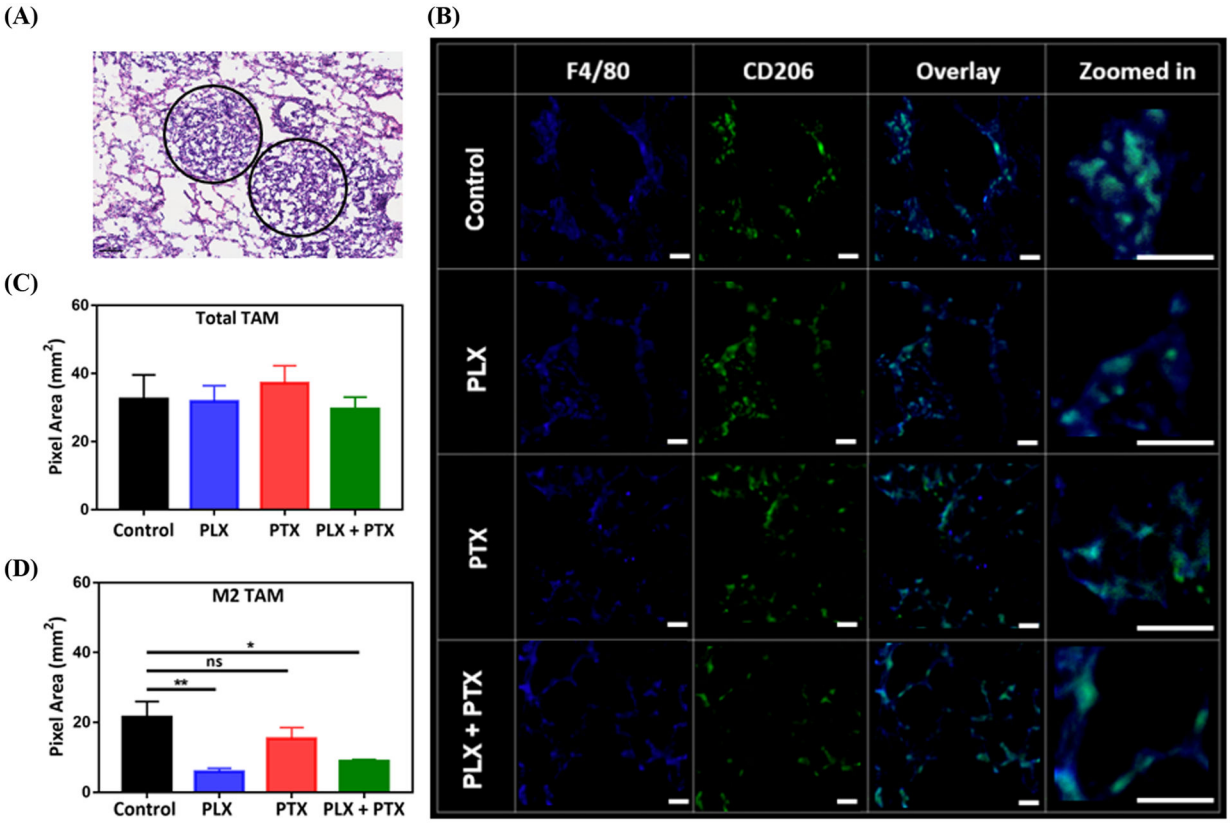

Figure 3.

PLX reduces the number of M2 TAM in the TME of 4T1 lung lesions. **(A)** Regions of 4T1 lung tumor nodules (circled), obtained by H&E staining of Balb/c lung tissue, **(B)** representative IF images acquired by confocal microscopy for total TAM ($F4/80^+$), $CD206^+$, and M2 TAM ($F4/80^+$ $CD206^+$ overlay, with zoomed in regions-"bluish green" represents overlay), **(C)** effect of PLX (p.a.) +/− PTX (i.v.), 1 mg/kg each, on total TAM population, **(D)** impact of therapy on M2 TAM. Tumors were collected from animal lungs (n=3) and six random images were taken on each group sample, pixels for total TAM and M2 TAM were converted to area (1pixel = 0.98 μm^2) and plotted in (C) and (D). PLX +/− PTX treated groups were compared with control and statistical significance was calculated by One-way ANOVA (*p <0.05, **p <0.01), data represented as mean ±SEM.

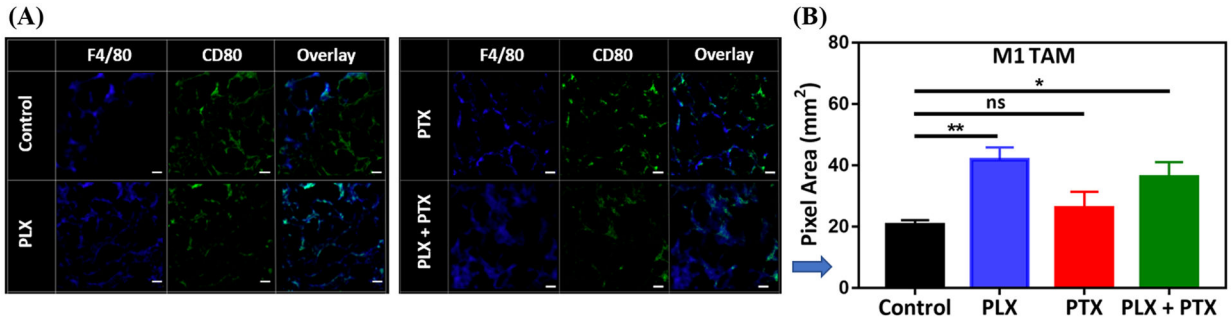

Figure 4.

PLX increases the number of M1 TAM in the TME of 4T1 lung lesions. **(A)** a representative IF image acquired by confocal microscopy for total TAM ($F4/80^+$), $CD80^+$, and M1 TAM ($F4/80^+$ $CD80^+$ overlay), **(B)** impact of PLX (p.a.) +/− PTX (i.v.), 1 mg/kg each, on M1 TAM. Tumor nodules were collected from animal lungs (n=3) and six random images were taken on each group sample, pixels for M1 TAM were converted to area (1pixel = 0.98 μm^2) and plotted in (B). PLX +/− PTX treated groups were compared with control and statistical significance was calculated by One-way ANOVA (*p <0.05, **p <0.01), data represented as mean ±SEM.

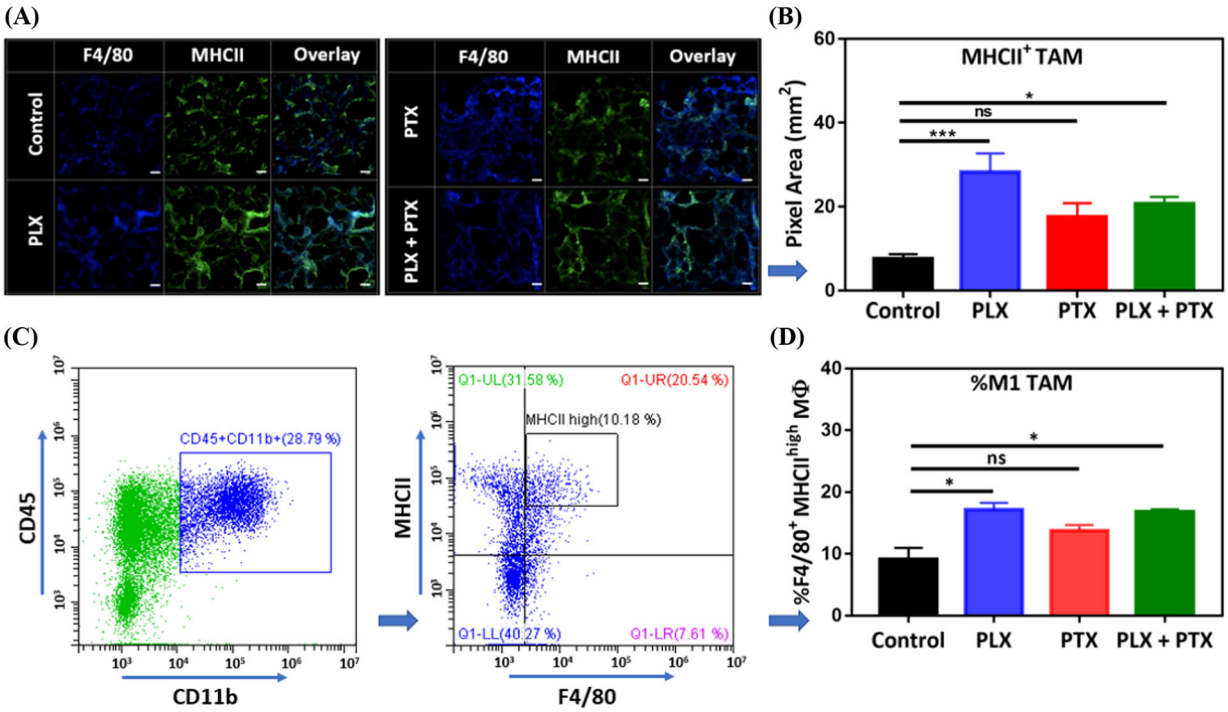

Figure 5.

PLX increases the population of MHCII$^+$ TAM in the TME of 4T1 lung lesions. **(A)** A representative IF image acquired by confocal microscopy for total TAM (F4/80$^+$), MHCII$^+$, and MHCII$^+$ TAM (F4/80$^+$ MHCII$^+$ overlay), **(B)** impact of PLX (p.a.) +/− PTX (i.v.), 1 mg/kg each, on MHCII$^+$ TAM population, obtained from (A). Tumor nodules were collected from animal lungs (n=3) and six random images were taken on each group sample, pixels for MHCII$^+$ TAM were converted to area (1pixel = 0.98 μm^2) and plotted in (B). **(C)** Gating strategy on Flow-cytometry for tumor samples (control group), M1 TAM are represented by CD45$^+$ CD11b$^+$ F4/80$^+$ MHCII^{high} cells, **(D)** effect of PLX (p.a.) +/− PTX (i.v.), 1 mg/kg each, on M1 TAM population obtained from (C) showing % of M1 TAM/CD45$^+$ CD11b$^+$. For (B) and (D), PLX +/− PTX treated groups were compared with control and statistical significance was calculated by One-way ANOVA (*p <0.05, ***p <0.001), data represented as mean ±SEM.